Infrared Cloud Imager Measurements of Cloud Statistics from the 2003 Cloudiness Intercomparison Campaign

B. Thurairajah and J. A. Shaw
Department of Electrical and Computer Engineering
Montana State University
Bozeman, Montana

Introduction

The Cloudiness Inter-Comparison Intensive Operational Period (CIC IOP) occurred at the Atmospheric Radiation Measurement (ARM), Southern Great Plains (SGP) central facility site in Lamont, Oklahoma from mid-February to mid-April 2003 (Kassianov et al. 2004). Two objectives of this IOP were to study and compare cloudiness measured by different instruments and to evaluate the capabilities of thermal infrared sensors, particularly for providing consistent day-night measurements. One of the thermal imagers deployed was the Infrared Cloud Imager (ICI), which identifies clouds and cloud type directly from the downwelling atmospheric radiance. ICI has been successfully deployed in the Arctic during previous years (Shaw and Thurairajah 2003, 2002; Westwater et al. 2004), and this deployment in the mid-latitude plains has been valuable for evaluating ICI's performance in a more humid atmosphere.

ICI Measurements at the CIC

The ICI is a thermal infrared imaging system that measures clouds from the downwelling atmospheric radiance or brightness temperature in the 8-14 μm spectral band. The measurements are radiometrically calibrated images of the band-integrated downwelling emission, from which the sky condition is determined at each pixel. The main components of the ICI system are an infrared camera that employs an uncooled microbolometer detector array, a blackbody source (two blackbody sources in the recently modified ICI system), a gold-coated beam-steering mirror, and control electronics (Shaw et al. 2002). The ICI was deployed in Lamont, Oklahoma as part of the CIC-IOP and collected data from February 20, 2003 to April 25, 2003. Since the system was originally built to withstand the cold Arctic climate, cooling fans had to be installed for the mid-latitude deployment.

The measurements taken by ICI include the downwelling radiance from both clouds, if present, and atmospheric gases. The main atmospheric gases contributing to the total emission in the 8-14 μm band are water vapor, ozone, and carbon dioxide (primarily water vapor). To identify clouds and calculate cloud statistics, the radiance of water vapor emission has to be removed (emission by other gases contribute little to our measured value and do not change significantly), leaving us with only the cloud radiance. In a warm region like the mid-latitude plains, where surface temperatures are widely varying, we found that it is important to include a surface-temperature dependence in estimating the water vapor emission. To remove the water vapor emission, a temperature-dependant water vapor correction was

identified from radiative transfer calculations using different MODTRAN atmospheric models. To process ICI data from the CIC deployment, we developed four equations relating integrated radiance to precipitable water vapor, at surface temperatures of approximately +27, +15, 0, and -15°C, and interpolated between them to determine the appropriate water vapor radiance correction. Figure 1 is a somewhat humorous ICI image from the CIC deployment, showing thin clouds and a flock of birds over the SGP site, color coded in terms of residual radiance (i.e., radiance after removing emission due to water vapor). Figure 2 shows another example ICI image, (a) before and (b) after water vapor correction. This temperature-dependant water vapor correction allowed us to see cirrus clouds located at 8-10 km AGL, through a precipitable water vapor amount of about 1.0 cm.

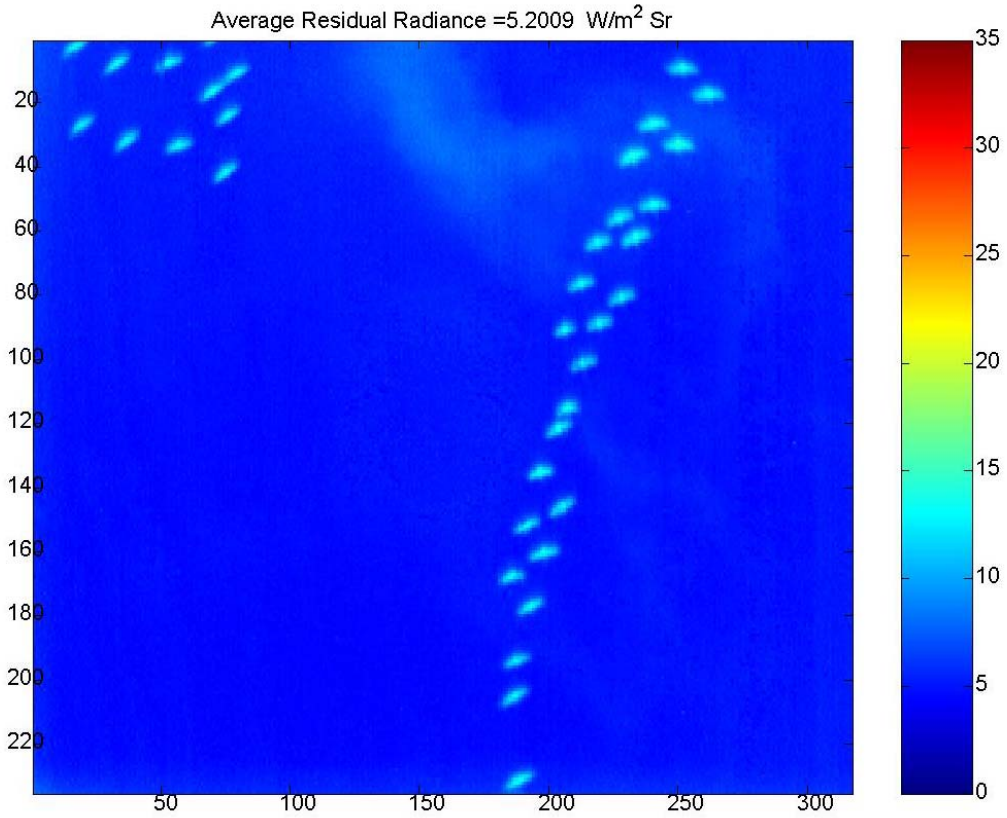

Figure 1. ICI image of thin clouds and a serendipitous flock of birds, seen at 1630 UTC on April 13, 2003, at Lamont, Oklahoma. The image is color coded in units of residual radiance, after removing emission from 2.4 cm of water vapor, color coded with blue representing clear-sky and red representing low-level clouds.

Cloud Statistics

After water vapor correction, we pass the residual radiance images through a threshold filter to identify each pixel as cloudy or clear (the magnitude of the residual radiance also can be used to make further classification of general cloud type). The initial threshold was determined from uncertainty estimates for the ICI radiometric calibration. We evaluated the threshold data by comparing the ICI cloud

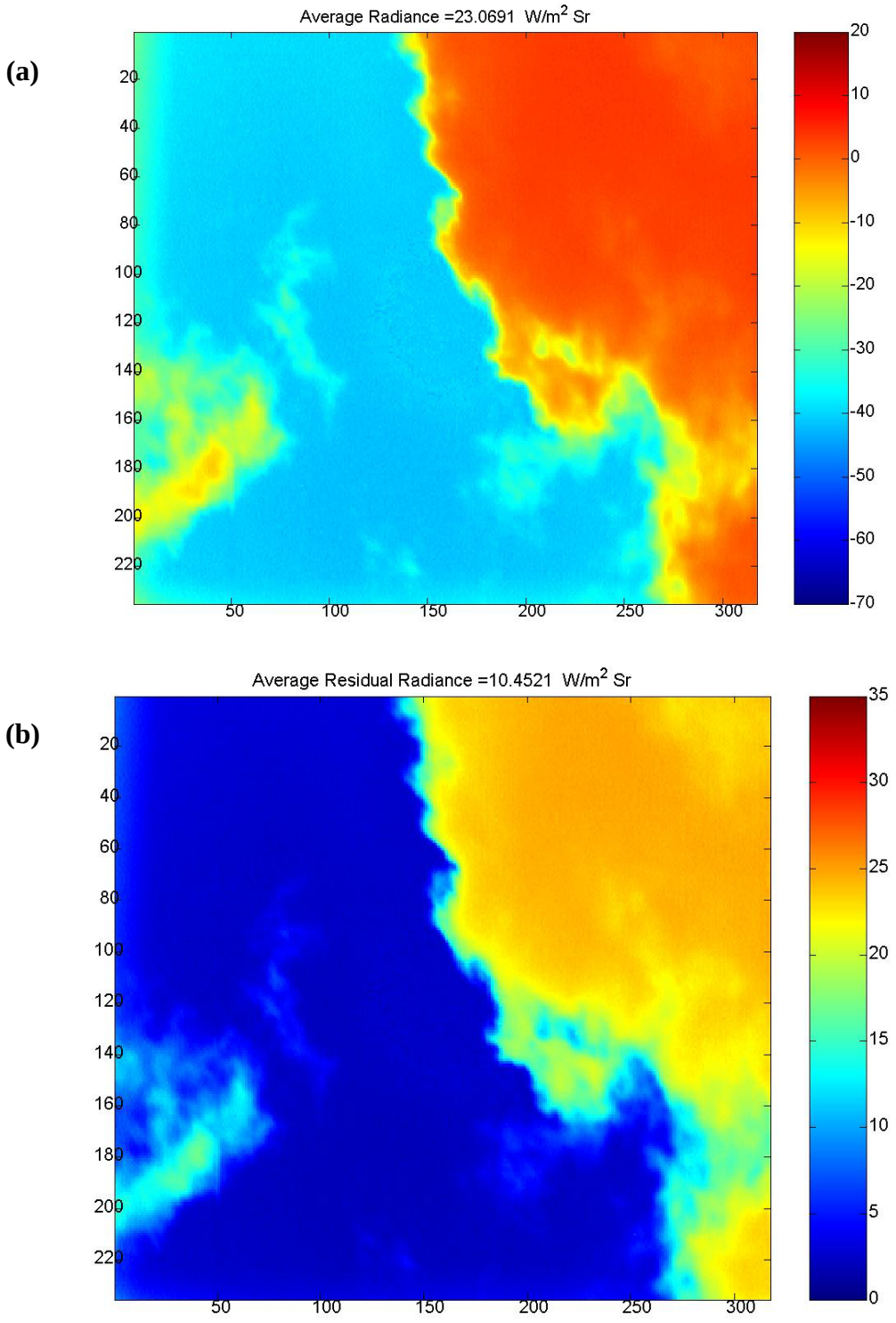

Figure 2. ICI images of clear-sky and clouds before and after water vapor correction, measured at 1943 UTC on April 20, 2003. Note that the average radiance decreases from 23.07 to 10.45 W/(m^2 sr) (a) before water vapor correction (color coded in brightness temperature units of K), (b) after water vapor correction (color coded in radiance units of W m^{-2} sr^{-1}).

amount (percentage of image containing clouds) to a corresponding temporal average of cloud amount measured by the vertically viewing micropulse lidar (MPL), and adjusted the threshold value to evaluate the ICI capability of detecting thin cirrus and other challenging conditions (we chose to use the MPL as a comparison basis specifically because of its high sensitivity to thin cirrus). An overall "best-initial-estimate" threshold was determined to be 2.65 W/(m^2 sr), which was used for an initial estimate of cloud statistics based on the fraction of an ICI image that is cloudy; i.e., the percentage of pixels with a radiance greater than the threshold. Figure 3 shows the resulting monthly cloud statistics histogram for the entire CIC dataset, with 0-10% representing clear-sky and the other bins representing the frequency of occurrence of clouds in an entire image. The overall statistics show that both March and April were approximately 50% cloudy, and that the skies tended to be predominantly mostly clear or mostly cloudy. The monthly frequency of sky cover derived from the value-added product of the broadband shortwave radiometers used at the SGP site show that over a period of six years from 1996 to 2001, the monthly overcast sky varied from 45 to 25% for both March and April (Gaustad and Long 2002) and the trend of seeing mostly clear and/or cloudy skies is similar to what is seen by the ICI.

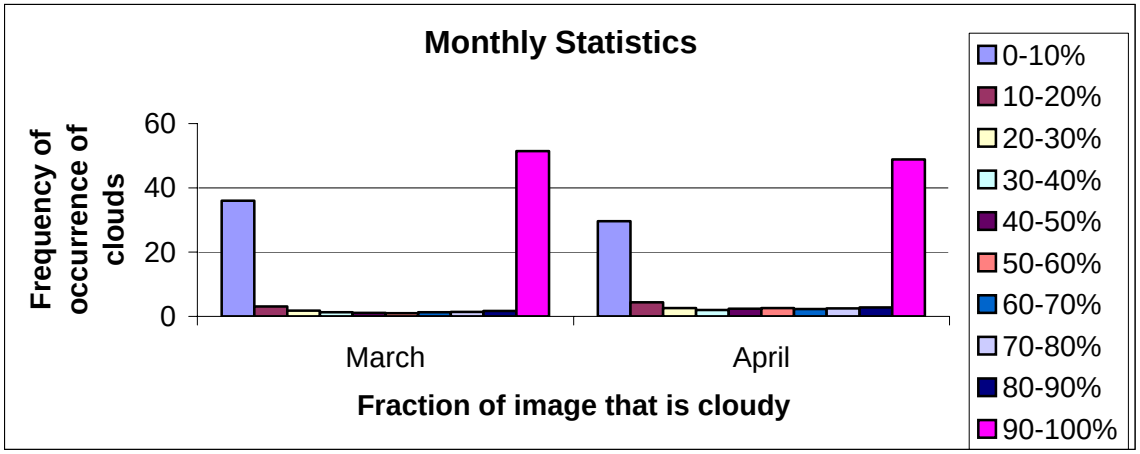

Figure 3. Monthly cloud statistics for March and April 2003, derived from ICI images processed with a constant threshold of 2.65 W m^{-2} sr^{-1}, for the entire duration of the CIC deployment.

Sometimes using a constant threshold to process data over long periods of time fails to detect thin clouds that have a radiance value lesser than the threshold, and at other times the constant threshold can identify emission due to haze as clouds. Recently, Turner and Long (2004) discussed the possibility that low-level haze, seen especially often during night and early mornings at the SGP site, increases the downwelling longwave flux, which may be related to the hazy pseudo-cloud signature we see in ICI data some of the time at SGP. Thus a constant threshold can either underestimate or overestimate cloudiness. A solution to this problem is to use adaptive thresholds that identify thin clouds and minimize the possibility of classifying haze as clouds. Preliminary results of ICI cloud amount computed with variable thresholds for selective days are promising. Scatter-plot comparisons of ICI cloud amount and MPL cloud amount are shown in Figure 4 for (a) a constant threshold of 2.65 and (b) variable threshold, determined using parameters such as the ICI residual radiance mean and variance, as well as ancillary data such as MPL cirrus detection. The correlation of ICI and MPL cloud amount improves noticeably when variable thresholds are used to identify clouds in ICI images. Further analysis also has shown that that the correlation between ICI and MPL is consistent between day and night, but that the correlation

(a)

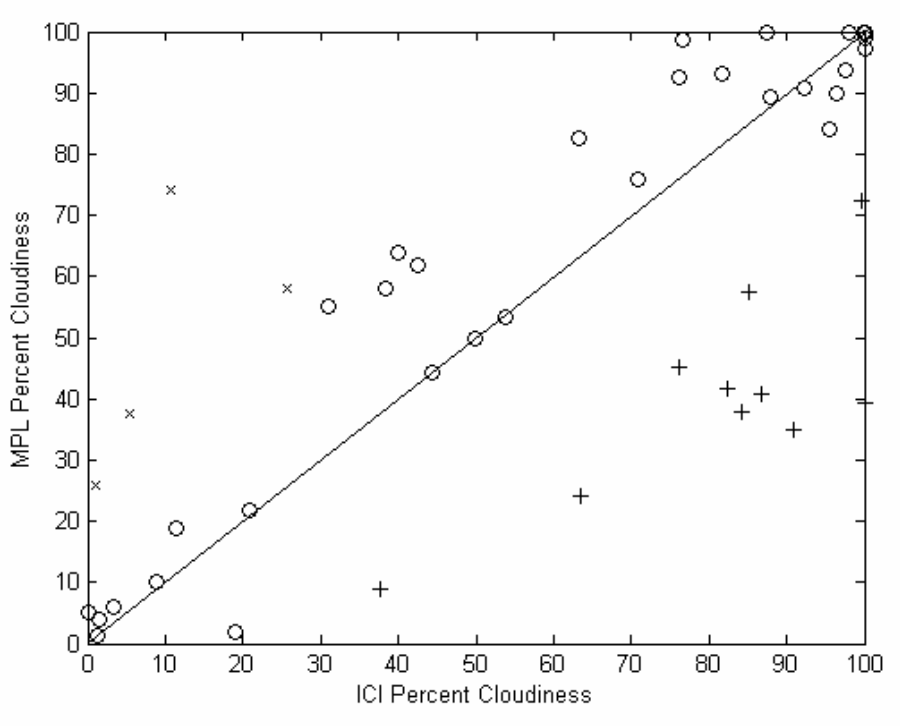

(b)

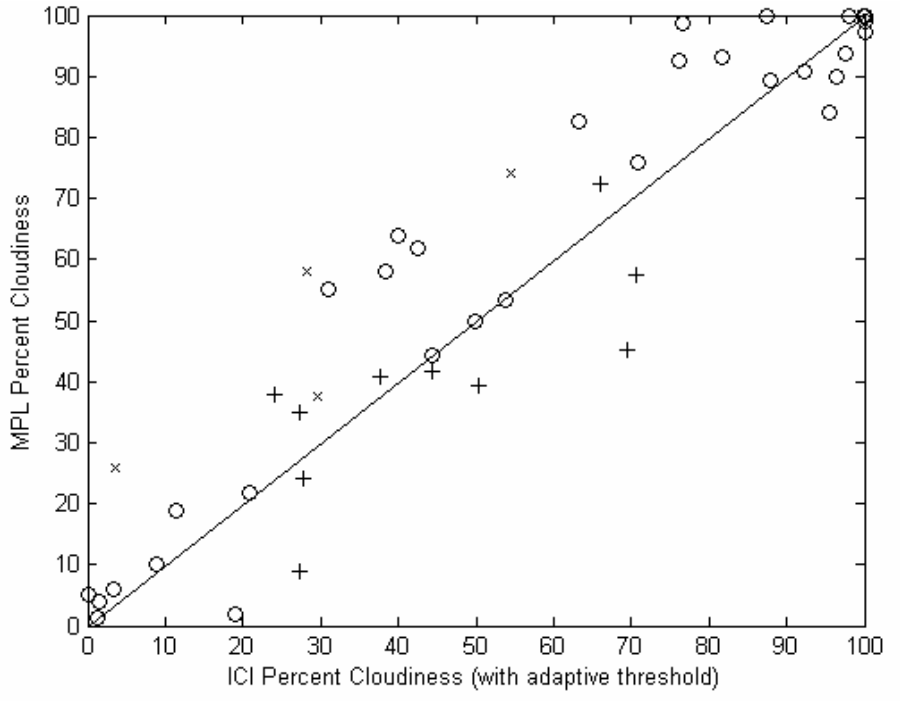

Figure 4. Scatter plot of ICI and MPL cloud amount (47 data points) with (a) constant threshold of 2.65 W/m^{-1} sr^{-1} (correlation coefficient = 0.752, RMS difference = 24.50) and (b) variable thresholds used to identify clouds for the cirrus and haze days marked with 'x' and '+', respectively (correlation coefficient = 0.937, RMS difference = 12.45).

between ICI and the whole sky imager (WSI) is degraded significantly at night when the WSI operates in star-viewing mode (Thurairajah and Shaw 2004). The ICI data, therefore, agrees with MPL data in a reasonable and encouraging fashion, but provides additional information about the horizontal cloud distribution that cannot be captured in zenith MPL data alone.

Conclusion and Future Work

Deploying ICI at SGP, together with several deployments in the Arctic, have helped us develop ICI into a more robust system that is capable of surviving both warm and cold climates. The analysis of ICI data from SGP has demonstrated that ICI is capable of determining reliable and consistent day-night measurements. Future data processing methods will incorporate automated algorithms that use adaptive thresholds to identify clouds. Further comparisons of ICI cloud statistics with results obtained from other sensors deployed during the CIC will help illuminate differences in detection capability for a variety of point and imaging cloud sensors.

The Infrared Cloud Imager was most recently deployed at the ARM North Slope of Alaska (NSA) site in Barrow, Alaska (Westwater et al. 2004), where it operated without interruption for five weeks during March-April 2004. The present ICI system has two blackbodies, instead of the previous one blackbody, to reduce much of the pixel-to-pixel variation and calibration uncertainty. Future versions of ICI will have wide angle imaging capability to obtain cloud cover within a significant fraction of the full sky.

Acknowledgement

This research was supported by the Office of Biological and Environmental Research of the U.S. Department of Energy as part of the Atmospheric Radiation Measurement Program. We gratefully acknowledge the valuable contributions to the successful deployment made by the operations staff at the ARM Southern Great Plains site.

Corresponding Author

B. Thurairajah, brentha_t@yahoo.com, (406) 994-7296

References

Gaustad, K. L., and C. N. Long, 2002: An evaluation of cloud cover, cloud effect, and surface radiation budgets at the SGP and TWP ARM sites. In *Proceedings of the Twelfth Atmospheric Radiation Measurement (ARM) Science Team Meeting*, ARM-CONF-2002. U.S. Department of Energy, Washington, D.C. Available URL: http://www.arm.gov/publications/proceedings/conf12/extended_abs/gaustad-kl.pdf

Kassianov, E., C. Long, and M. Ovtchinnikov, 2004: ARM cloudiness intercomparison IOP 2003 analysis: Sky Cover and Cloud Fraction. This Proceedings.

Shaw, J. A, B. Thurairajah, and E. Edqvist, 2002: Infrared Cloud Imager deployment at the North Slope of Alaska during early 2002. In *Proceedings of the Twelfth Atmospheric Radiation Measurement (ARM) Science Team Meeting*, ARM-CONF-2002. U.S. Department of Energy, Washington, D.C. Available URL: http://www.arm.gov/publications/proceedings/conf12/extended_abs/shaw-ja.pdf

Shaw, J. A., and B. Thurairajah, 2003: Short-term Arctic cloud statistics at NSA from the Infrared Cloud Image. In *Proceedings of the Thirteenth Atmospheric Radiation Measurement (ARM) Science Team Meeting*, ARM-CONF-2003. U.S. Department of Energy, Washington, D.C. Available URL: http://www.arm.gov/publications/proceedings/conf13/extended_abs/shaw-ja.pdf

Thurairajah, B., and J. A. Shaw, 2004: Cloud statistics measured with the Infrared Cloud Imager. *IEEE Trans. Geosci. Rem. Sens.*, submitted.

Turner, D. D., and C. N. Long, 2004: Direct aerosol forcing in the infrared at the SGP site? This Proceedings. Available URL: http://www.arm.gov/publications/proceedings/conf14/extended_abs/turner-dd.pdf

Westwater, E. R., M. Klein, A. Gasiewski, V. Leuski, J. A. Shaw, V. Mattioli, D. Cimini, J. C. Liljegren, B. M. Lesht, and B. D. Zak, 2004: The 2004 North Slope of Alaska winter radiometric experiment. This Proceedings.